STATISTICS, OPTIMIZATION AND INFORMATION COMPUTING
Stat., Optim. Inf. Comput., Vol. **x**, Month 202x, pp 0–11.
Published online in International Academic Press (www.IAPress.org)

A Novel Dmey Wavelet Charts for Controlling and Monitoring the Average and Variance of Quality Characteristics

Talal Abd Al-Razzaq Saead Al-Hasso [1], Mahmood M Taher [1,*], Taha Hussein Ali[2]

[1]*Department of Statistics and Informatics, University of Mosul, Iraq*
[2]*Department of Statistics and Informatics, Salahaddin University, Iraq*

Abstract Shewhart charts for quality control of the average and variance of quality characteristics and their monitoring can be affected by data noise. This article proposes the creation of novel charts based on wavelet analysis, specifically the Dmey wavelet, to handle data noise. The discrete wavelet transformation of the Dmey wavelet, which divides the data into two halves, is the foundation of the suggested charts. In contrast, the detail coefficients are proportional to the variance of the observations or the differences between the observations. Through them, the D chart is constructed, which corresponds to the Shewhart chart for the variance. The approximation coefficients are proportional to the average of the observations, and through them the A chart is constructed, which corresponds to the Shewhart chart for the average. Both simulated data and actual data about the weights of infants at Valia Hospital in Erbil were utilized to illustrate the effectiveness of the suggested charts and compare them with Shewhart charts. According to the simulation results, the weights of the infants at Valia Hospital were under control, the suggested charts were effective at treating noise, and were more responsive to even small changes in the Shewhart charts' quality attributes.

Keywords Quality Control Charts, Average Chart, Variance Chart, Dmey Wavelet, Approximate and Detail Coefficients

DOI: 10.19139/soic-2310-5070-2621

1. Introduction

Based on the idea of identifying departures from statistically permissible bounds, statistical quality control for Shewhart charts keeps track of the average and variance of quality characteristics in different processes. However, the quality of the data utilized has a major impact on the accuracy and efficacy of these charts, since noisy data produces inaccurate results and, in turn, wrong decisions that can have a detrimental impact on the production or service process.

New research trends that seek to integrate wavelet analysis techniques into statistical quality control have been sparked by recent developments in signal and data processing technologies. Wavelet analysis efficiently handles noisy data to obtain insightful information, as numerous studies have demonstrated. For example, researchers [17] used wavelet analysis to improve detection performance by removing noise. Within modified multivariate control schemes, they used specific wavelengths and concentrated on three statistics: variance, mean, and standard deviation. Similarly, to determine congestion conditions, the researchers [18] used an exponentially weighted uncorrelated moving average control approach. Their results show that the use of this statistical method to monitor vehicle traffic has improved significantly.

In [4] wavelet-based techniques for K-process monitoring were introduced, in the same year, researchers created [19] time series difference equation models and multiple regression models to identify common causes of

*Correspondence to: Mahmood M Taher (Email: mahmood81_tahr@uomosul.edu.iq).Department of Statistics and Informatics, College of Computer Science and Mathematics, University of Mosul, Nineveh, Iraq.

ISSN 2310-5070 (online) ISSN 2311-004X (print)

variations in monitoring data. Then, to identify variances, individual control plots, moving range control plots, and exponentially weighted moving average control plots were created. The hybrid wavelet strategy, which employs wavelet analysis to remove noise and outliers from data, was simultaneously proposed by researchers [11]. The outcomes demonstrate how much power indices are improved by the suggested strategy. The results demonstrate how wavelet analysis can greatly increase precision and productivity, which will improve the quality control of manufacturing processes.

To develop new monitoring techniques that can better handle data noise, this study offers a novel concept based on the application of the Dmey wavelet. The Dmey wavelet, which combines the benefits of Daubechies and Meyer wavelets, was specially selected because of its unique characteristics in assessing unstable signals.

The discrete wavelet transformation (DWT), which divides the data into two primary sections, detail coefficients associated with the variance of quality attributes and approximation coefficients associated with the mean of these qualities, is the foundation of the suggested charts. Scheme A, which is equivalent to the Shewhart mean scheme, and Scheme D, which is equivalent to the Shewhart variance scheme, were developed using these two kinds of coefficients.

A thorough simulation analysis was carried out to compare the performance of the suggested charts with that of conventional Shewhart schemes under varied noise situations to demonstrate their effectiveness. To show how applicable these schemes are in practical settings, they were also used on actual data that represented the weights of babies at Valia Hospital in Erbil.

The purpose of this article is to aid in the creation of more precise and useful instruments for process quality monitoring in the face of data noise, enabling businesses to make more trustworthy and accurate quality management decisions.

2. Quality Control Charts

Tools used in manufacturing to track and execute operations within a specific time range are called statistical quality control charts. They are well-focused in identifying variations or anomalies in a process that may lead to errors or deviations from what is expected [1]. These charts generally provide plotted data points in conjunction with control limits that indicate the expected variation within the process [8]. Data points that go up certain thresholds or show non-random patterns suggest that the process may be uncontrolled, warranting additional scrutiny and remedial measures. Quality control charts guarantee consistent product quality and enhance processes [14].

3. Average Chart

The average chart is used to control the average level of the specific property of the material produced, and the points drawn on this chart are the rate per sample compared to the number of samples (or time) [3] [2].

The target line is the general average. $\mathrm{T} = \overset{?}{\mathrm{X}}$ For all arithmetic means calculated and taken from the production line for a long time (Kareem et al. 2019) [6]. As for the control limits, they are calculated as follows:

$$\begin{matrix}\mathrm{UCL} \\ \mathrm{LCL}\end{matrix}\begin{pmatrix}\bar{\bar{X}} \\ \bar{\bar{X}}\end{pmatrix} = \bar{X} \pm 3 \times \sigma_{\bar{\mathrm{X}}} \tag{1}$$

Whereas: $\overset{?}{\mathrm{X}} = \sum_{j=1}^{m} \bar{\mathrm{X}}_j / m$, $\bar{\mathrm{X}}_j = \sum_{i=1}^{n} x_{ij}/n$. The standard deviation of the sample means is:

$$\sigma_{\bar{\mathrm{X}}} = \sqrt{\sum_{j=1}^{m} \left(\bar{\mathrm{X}}_j - \bar{\bar{X}}\right)^2 / (m-1)}$$

4. Variance Chart

The variance chart allows us to study the stability of the production process to a change if the field of change is almost constant over time and the deviation chart requires its results, and this standard stability is achieved that the number of selected samples is K (k $\geq$ 9), but if the number of samples is k $\leq$ 9 We use the range chart (Sakar et al. 2024) [12].

The Target (Mean of Variance) is $\overline{s^2}$. The UCL and LCL for the variance chart are calculated using the mean and standard deviation of the sample variances [16]:

$$\begin{matrix} \text{UCL} \\ \text{LCL} \end{matrix} \begin{pmatrix} s^2 \\ s^2 \end{pmatrix} = \overline{s^2} \pm 3 \times \sigma_{s^2} \tag{2}$$

If the calculated LCL for variance is negative, set it to 0 because variance cannot be negative.

5. Dmey Wavelet

Dmey is a discrete wavelet derived from the continuous Meyer wavelet, which is a semi-orthogonal wavelet. It has ideal properties in the frequency domain, making it suitable for multi-resolution signal analysis, and it has better symmetry than the traditional Daubechies wavelet. It is a type of mathematical wavelet used in signal processing and data analysis.

This wavelet combines the work of Ingrid Daubechies and Yves Meyer and incorporates properties from Daubechies and Meyer waves [10].

6. Discrete waveform transformation

Discrete waveform transformation (DWT) is one of the most widespread techniques in the field of wavelet analysis due to its multiple practical and theoretical applications in various scientific fields [13].

The discrete wavelet transform is based on Mallat's hierarchical algorithm, an efficient algorithm proposed by Mallat in 1989, as referred to by (Nason ,2008) [9], to extract wavelet coefficients from data sets containing noise. The mechanism of this algorithm is based on creating smooth and contrast filters based on the wavelet coefficients, where these filters are applied repeatedly to obtain data at different scales.Thus,the wavelet transforms the data into two main components: The first component is known in detail and includes high frequencies that can be calculated from the parent waves according to the formula referred to by [15]; [5].

$$\psi(x) = \sum\nolimits_r S(r) \sqrt{2} \varphi(2x - r) \qquad \text{r} \ , \ \in \text{Z} \tag{3}$$

Whereas
S : The second component is known as the approximate component and includes low frequencies (noise) or outliers, depending on the study's nature and field of application. This component of the father wave can be calculated according to the formula provided by [5], where it acts as a filter for high frequencies, as they indicated in their study.

$$\emptyset(x) = \sum_r f(r) \sqrt{2} \varphi(2x - r) \qquad , \qquad r \in Z \tag{4}$$

While f : Stands for the low-pass filter, as explained by [5]. This filter is related to $S(r)$ Through a specific relationship.

$$f(r) = (-1)^r S(r) \tag{5}$$

7. Proposed Charts

The proposed method presented novel quality control charts based on wavelet analysis of the approximation and detail coefficients of the Dmey wavelet corresponding to the Shewhart chart for the average and variance, as follows:
Suppose x_{j} is a data vector representing many samples (m). Perform a DWT for the Dmey wavelet for the data vector and produce m/2 + 50 if m is even and (m+1)/2 + 50 (50 is a constant value for the Dmey wavelet) of the approximate and detail coefficients (two partitions) are in formulas 6 and 7. After padding, the DWT splits the data into approximation and detail coefficients. The padding length and the implementation of the DWT algorithm influence the final number of coefficients.

$$\mathrm{Aj}\,[\mathrm{m}] = \sum\nolimits_{k=0}^{1} h\,[k] \times x_{\mathrm{j}}\,[2m-k] \tag{6}$$

$$\mathrm{Dj}\,[\mathrm{m}] = \sum\nolimits_{k=0}^{1} g\,[k] \times x_{\mathrm{j}}\,[2m-k] \tag{7}$$

For j = 1, 2, …, n represent many observations in the sub-sample. Here, take every second sample of the data (downsampling by a factor of 2) to compute the approximation and detail coefficients where m varies over the appropriate indices of the data. Formula 6 represents the approximation coefficients (first part), scale or father function Aj[m] and with (m/2 + 50) if m is even and ((m+1)/2 + 50) coefficients, which are proportional to the qualitative characteristics of average observations and $h\,[k]$ represent low-pass filter for approximate coefficients:

$$h\,[0] = \left[\frac{1+\sqrt{3}}{4}\right],\ h\,[1] = \left[\frac{3+\sqrt{3}}{4}\right]$$

In contrast, formula 7 represents (second part) the detail coefficients Dj[m], the mother or wavelet function with the same number of approximate coefficients, which are proportional to the variance of the observations of the qualitative characteristic and $g\,[k]$ represent high-pass filter for approximate coefficients:

$$g\,[0] = \left[\frac{-1+\sqrt{3}}{4}\right],\ g\,[1] = \left[\frac{3-\sqrt{3}}{4}\right]$$

The approximation and detail coefficients are converted to normal vectors by dividing them by $(\sqrt{2})$ to get Aj and Dj, respectively, which orthogonal wavelets to maintain the signal's total energy during reconstruction. Where A = [A_1 A_2 … A_n] and D = [D_1 D_2 … D_n].

$$\bar{\mathrm{A}} = \sum\nolimits_{i}^{n} \mathrm{A}_i/n \tag{8}$$

$$\bar{\mathrm{D}} = \sum\nolimits_{i}^{n} \mathrm{D}_i/n \tag{9}$$

Where $\bar{\mathrm{A}}$ and $\bar{\mathrm{D}}$ are a mean vector of approximate and detail coefficients, respectively.

The proposed charts are based on the Dmey wavelet analysis, which involves creating two charts, the first for controlling the Dmey wavelet approximation coefficients $(\bar{\mathrm{A}}_{\mathrm{j}})$ for the observations average, which represents the plotted points on the approximate Dmey chart (A Chart), and the second for controlling the Dmey wavelet detail coefficients $(\bar{\mathrm{D}}_{\mathrm{j}})$ for the variance of the observations (Difference), which represents the plotted points on detail Dmey chart (D Chart). Target Lines for A Chart and D Chart respectively are:

$$\text{Tartget Line } (\mathrm{A}) = \sum\nolimits_{\mathrm{j}=1}^{\mathrm{m}} \bar{\mathrm{A}}_{\mathrm{j}}/\mathrm{m} \tag{10}$$

$$\text{Tartget Line } (\mathrm{D}) = \sum\nolimits_{\mathrm{j}=1}^{\mathrm{m}} \bar{\mathrm{D}}_{\mathrm{j}}/\mathrm{m} \tag{11}$$

The upper and lower control limits for the A and D Charts respectively are:

$$\begin{matrix}\mathrm{UCL}\ (\mathrm{A}) \\ \mathrm{LCL}\ (\mathrm{A})\end{matrix} = \text{Target Line } (\mathrm{A}) \pm 3 \times \sigma_{\bar{\mathrm{A}}} \tag{12}$$

$$\begin{matrix}\text{UCL (D)}\\ \text{LCL (D)}\end{matrix} = \text{Target Line (D)} \pm 3 \times \sigma_{\bar{\text{D}}} \tag{13}$$

Where $\sigma_{\bar{\text{A}}}$ and $\sigma_{\bar{\text{D}}}$ represent the standard deviation for approximate and detailed Dmey coefficients, respectively. Note that when creating the proposed charts for the first time (Phase I), all the points drawn on them must be within the control limits. If several points fall outside the control limits, modified charts can be created for the A chart by replacing those values with the coefficients average and for the D chart by zeroing out the values that fall outside the control limits, i.e. applying the kill or keep rule.

8. Simulation Study

To evaluate the effectiveness of the proposed control charts and compare them with classical charts, begin by simulating data for an in-control process. In this case, we assume that the process is normally distributed with a known mean ($\mu = 100$) and standard deviation ($\sigma = 1$). The sample size is n = 5, meaning each sample contains 5 items.
The number of samples is m = 30, leading to a dataset with 30 groups of 5 items. The goal of this simulation is to model the natural variability of a process under ideal conditions, where the process is considered stable and free from any external disruptions.
Figure 1 shows the behaviour of the generated data for the first simulation experiment (data1, data2, ..., data5) with the DWT of the Dmey wavelet for this data which represents the behaviour of the approximation coefficients (low-pass filter) transformed to the normal coefficients (A1, A2, ..., A5) which are proportional to the observation average and the behaviour of the detail coefficients (high-pass filter) transformed to the normal coefficients (D1, D2, ..., D5) which are proportional to the observation variance or differences.

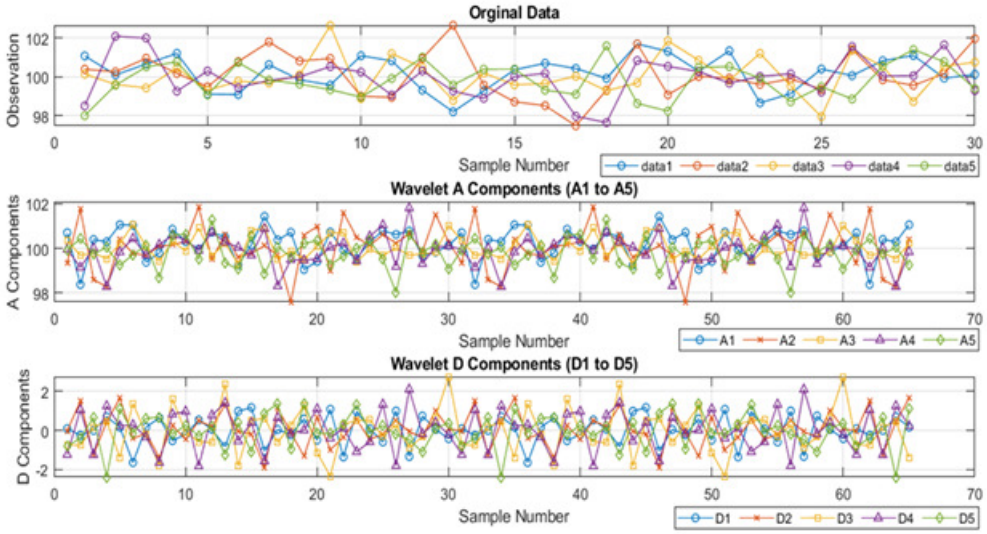

Figure 1. Wavelet Analysis for the First Simulation Experiment.

Figure 2 shows the classical Shewhart charts of the average and variance chart where the dots plotted on them represent the average and variance (blue), respectively, while the green represents the target line and the red the upper and lower control limits. All the points plotted on the two charts (Phase I) were within the control limits, so they can be relied upon to control and monitor the production process for average and variance in Phase II.

Figure 3 shows the proposed charts of the A and D charts where the dots plotted on them represent the approximate and detailed coefficients (blue), respectively, while the green represents the target line and the red

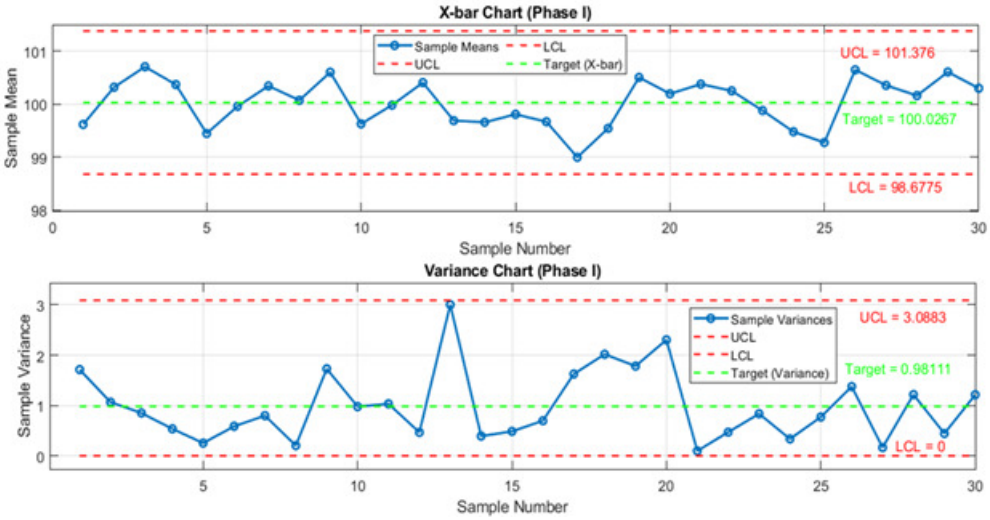

Figure 2. Classical Charts for the First Simulation Experiment.

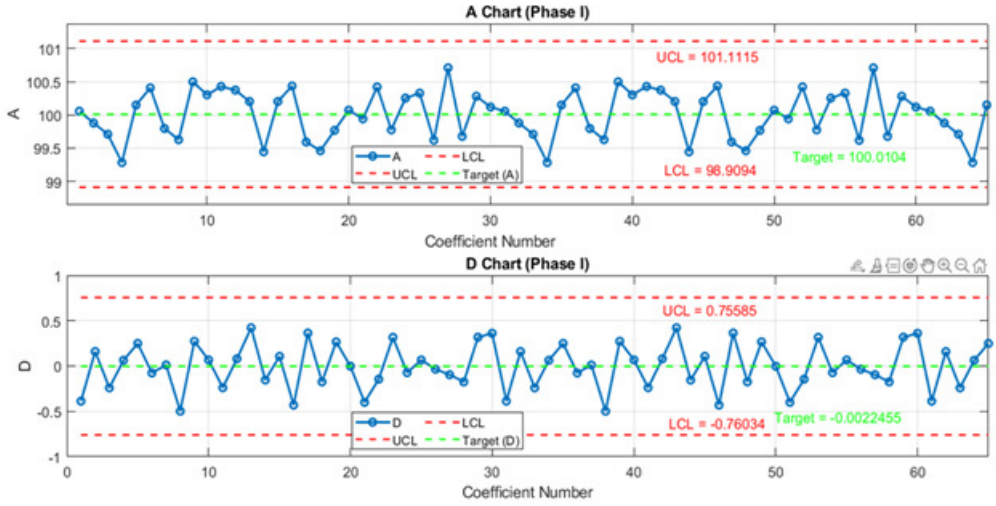

Figure 3. Proposed Charts for the First Simulation Experiment.

the upper and lower control limits. All the points plotted on the two charts (Phase I) were within the control limits, so they can be relied upon to control and monitor the production process for the average and difference in Phase II.

Table 1. Results of First Simulation Experiment

Chart	**UCL**	**LCL**	**Target**	**Sigma**	**Range (UCL-LCL)**
Classical X	101.3760	98.6775	100.0267	0.4498	2.6985
Classical Variance	3.0883	0.0000	0.9811	0.7024	3.0883
Proposed A	101.1115	98.9094	100.0104	0.3670	2.2020
Proposed D	0.7559	-0.7603	-0.0022	0.2527	1.5162

Table 1 shows that Classical $\bar{X}$ chart has control limits of 101.3760 (UCL) and 98.6775 (LCL), with the target set at 100.0267. The sigma (standard deviation) is 0.4498, and the difference between UCL and LCL is 2.6985. The classical variance chart has control limits of 3.0883 (UCL) and 0.0000 (LCL), with the target variance being 0.9811. The sigma is 0.7024, and the difference is 3.0883.

A chart has a narrower control limit range than the classical $\bar{X}$ and classical Variance charts, with a difference of 2.2020. The sigma = 0.3670 is smaller, which indicates less variability around the target, suggesting better control and process stability; thus, chart A is more efficient in controlling variability than the classical variance chart and classical $\bar{X}$ the chart is averaged.

The proposed D chart has the smallest control limit range for difference = 1.5162, indicating the tightest control over the process and denoise data. The sigma = 0.2527 is also the smallest, suggesting very low variability and high precision. This is the most stable chart in terms of variability and range, showing that the proposed D chart may be the most effective for achieving tight process control.

The simulation experiments were repeated 1000 times with different assumed parameters ($\mu = 100, 10$, and 5, $\sigma = 1, 2, 3$), different sample sizes (5 and 10), and different numbers of samples (30 and 25). Tables 2-4 explain the results of the classical ($\bar{X}$ and Variance) and proposed (A and D) charts.

Table 2. Classical and Proposed Charts (μ = 100 and Sigma = 1)

Chart	**n and m**	**UCL**	**LCL**	**Target**	**Sigma**	**Range (UCL-LCL)**
Classical $\bar{X}$	5 and 30	101.3334	98.6566	99.9950	0.4461	2.6768
Classical Variance		3.0823	0.0000	0.9963	0.6953	3.0823
Proposed A		100.9274	99.0626	99.9950	0.3108	1.8648
Proposed D		0.9283	-0.9283	0.0000	0.3094	1.8565
Classical $\bar{X}$	10 and 25	100.9339	99.0580	99.9959	0.3126	1.8759
Classical Variance		2.4046	0.0011	1.0044	0.4667	2.4035
Proposed A		100.9252	99.0622	99.9937	0.3105	1.8630
Proposed D		0.4654	-0.4646	0.0004	0.1550	0.9299

Table 3. Classical and Proposed Charts (μ = 10 and Sigma = 2)

Chart	**n and m**	**UCL**	**LCL**	**Target**	**Sigma**	**Range (UCL-LCL)**
Classical $\bar{X}$	5 and 30	12.6668	7.3133	9.9900	0.8923	5.3535
Classical Variance		12.3293	0.0000	3.9854	2.7813	12.3293
Proposed A		11.8549	8.1253	9.9901	0.6216	3.7296
Proposed D		1.8563	-1.8568	-0.0002	0.6188	3.7131
Classical $\bar{X}$	10 and 25	11.8677	8.1160	9.9919	0.6253	3.7518
Classical Variance		9.6184	0.0044	4.0176	1.8669	9.6140
Proposed A		11.8504	8.1243	9.9874	0.6210	3.7261
Proposed D		0.9306	-0.9292	0.0007	0.3100	1.8599

Classical $\bar{X}$ and the proposed charts in Table 2 show that they have the narrowest control limits and the smallest differences. However, the proposed A chart has a much smaller sigma, indicating tighter control and better process stability than the Classical $\bar{X}$ chart. The classical variance chart has a wider range and larger differences, indicating less control and higher variability. The proposed D chart also shows low variability and tighter control limits compared to the classical variance chart, although the range (difference) is slightly smaller for the proposed D chart.

Table 3 shows that the proposed A and D charts have significantly smaller differences in control limits, particularly the proposed D chart, which offers the tightest control. classical $\bar{X}$ chart still shows reasonable control,

Table 4. Classical and Proposed Charts (μ = 5 and Sigma = 3)

Chart	n and m	UCL	LCL	Target	Sigma	Range (UCL-LCL)
Classical $\bar{X}$	5 and 30	9.0002	0.9699	4.9851	1.3384	8.0303
Classical Variance		27.7410	0.0000	8.9671	6.2580	27.7410
Proposed A		7.7823	2.1879	4.9851	0.9324	5.5944
Proposed D		2.7844	-2.7852	-0.0004	0.9283	5.5696
Classical $\bar{X}$	10 and 25	7.8016	2.1739	4.9878	0.9379	5.6277
Classical Variance		21.6415	0.0099	9.0396	4.2006	21.6315
Proposed A		7.7756	2.1865	4.9811	0.9315	5.5891
Proposed D		1.3959	-1.3939	0.0010	0.4650	2.7898

but the classical variance chart shows high variability with large differences in control limits (12.3293), meaning it has less stability than the others. The proposed D chart has a very low sigma, suggesting very tight control and less variability than the other charts, especially the classical variance chart.

Table 4 shows that the classical variance chart has very high variability with the largest control limits and differences (27.7410), suggesting poor stability. The proposed A and D charts continue to show more controlled results. The proposed D has the smallest difference (2.7898), demonstrating its superior ability to minimize variability. The classical $\bar{X}$ shows a wide range in this scenario, with a difference of 8.0303, indicating less precise control over variability.

The proposed A and D charts are consistently better than the classical $\bar{X}$ and variance charts, showing tighter control limits and smaller differences between UCL and LCL. The proposed D generally provides the smallest control limit range and lowest sigma, indicating the tightest control across all conditions, which is ideal for achieving high precision.

The classical variance chart consistently shows wider control limits and higher variability, particularly at higher values of σ, suggesting it's less effective in tightly controlling variability. As the values of μ decrease (from 100 to 5) and σ increase (from 1 to 3), the performance difference becomes even more noticeable, with the proposed D chart remaining the most stable and precise.

9. Real Data

The real data represents the weights of newborns that were performed on 100 babies over two months at Valia Hospital in Erbil. The hospital has a specialized department for newborns and premature babies that operates 24 hours a day, seven days a week, supervised by specialist doctors to ensure the safety and care of newborns. Figure 4 shows the behaviour of the weights of newborns (data1, data2, . . . , data5) for m = 20 and n = 5 with the DWT of the Dmey wavelet for this data which represents the behaviour of the approximation coefficients (low-pass filter) transformed to the normal coefficients (A1, A2, . . . , A5) which are proportional to the observation average and the behaviour of the detail coefficients (high-pass filter) transformed to the normal coefficients (D1, D2, . . . , D5) which are proportional to the observation variance or differences.

Figure 5 shows the classical Shewhart charts of the average and variance chart where the dots plotted on them represent the average and variance (blue) for the weights of newborns, respectively, while the green represents the target line and the red the upper and lower control limits. All the points plotted on the two charts (Phase I) were within the control limits, so they can be relied upon to control and monitor the weights of newborns at Valia Hospital in Erbil for average and variance in Phase II.

Figure 6 shows the proposed charts of the A and D charts where the dots plotted on them represent the approximate and detail coefficients (blue) for the weights of newborns, respectively, while the green represents the target line and the red the upper and lower control limits. All the points plotted on the two charts (Phase I)

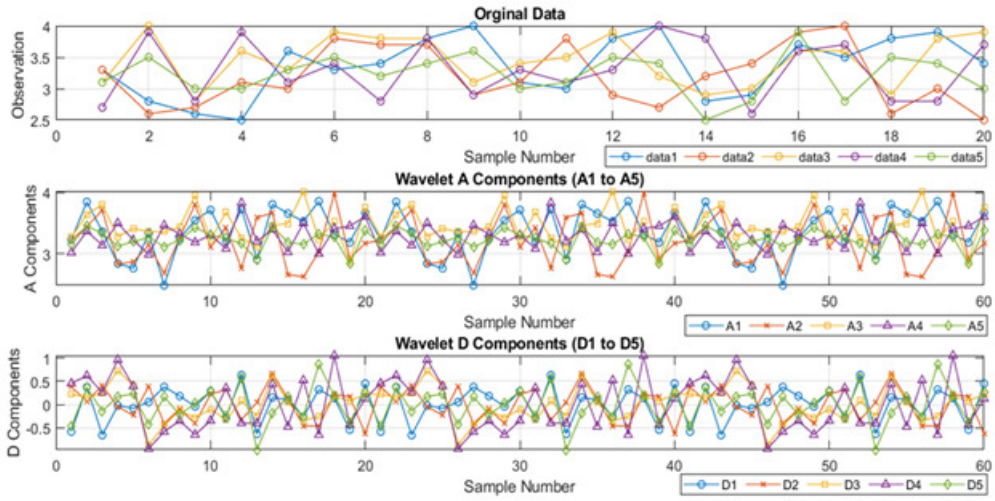

Figure 4. Wavelet Analysis for Real Data.

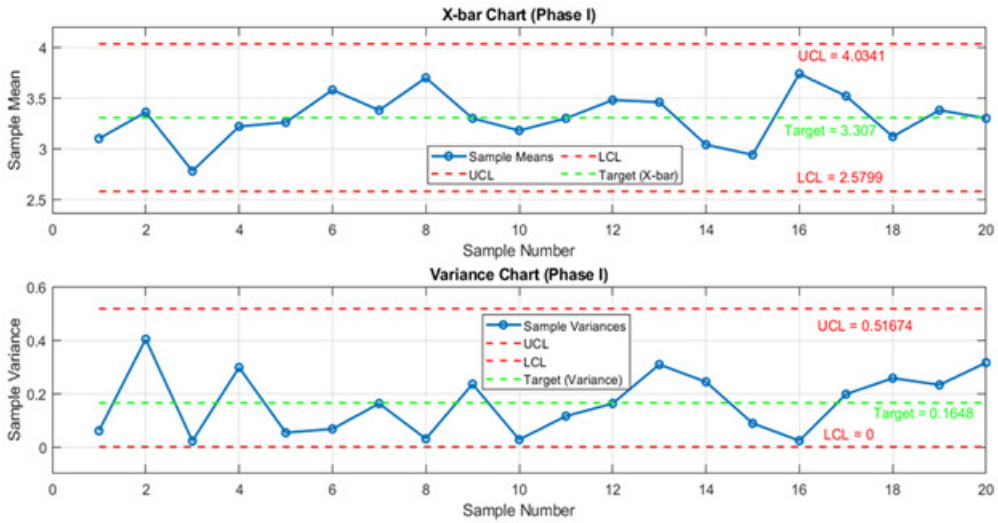

Figure 5. Classical Charts for Real Data (Phase I).

were within the control limits, so they can be relied upon to control and monitor the weights of newborns at Valia Hospital in Erbil for the average and difference in Phase II.

Table 5. Results of Real Data

Chart	UCL	LCL	Target	Sigma	Range (UCL-LCL)
Classical X̄	4.0341	2.5799	3.3070	0.2424	1.4543
Classical Variance	0.5167	0.0000	0.1648	0.1173	0.5167
Proposed A	3.8297	2.7843	3.3070	0.1742	1.0454
Proposed D	0.1219	-0.1219	0.0000	0.0406	0.2437

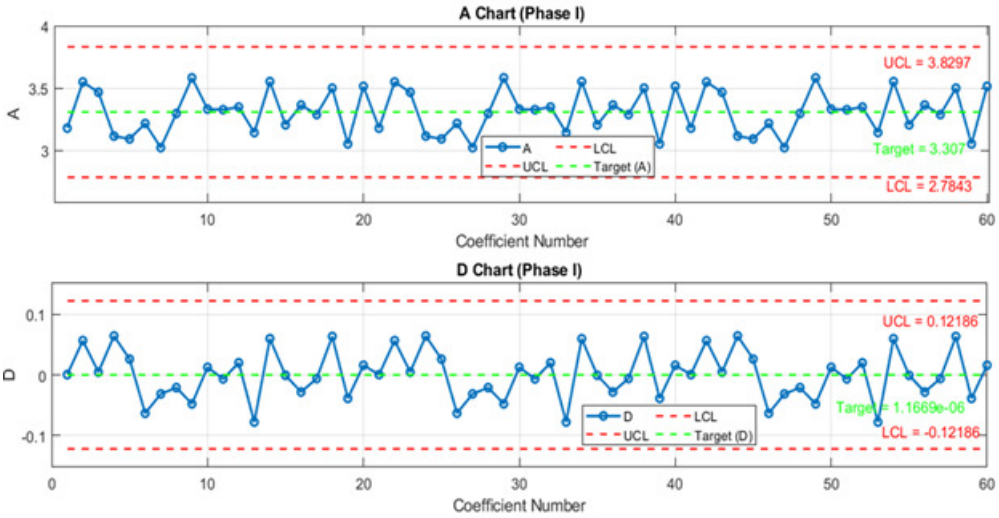

Figure 6. Proposed Charts for Real Data (Phase I).

Table 5 shows that the Classical $\bar{X}$ chart for weights of newborns has control limits of 4.0341 (UCL) and 2.5799 (LCL), with the target set at 3.3070. The sigma (standard deviation) is 0.2424, and the difference between UCL and LCL is 1.4543. The classical variance chart has control limits of 0.5167 (UCL) and 0.0000 (LCL), with the target variance being 0.1648. The Sigma = 0.1173, and the difference is 0.5167.

Weights of newborns have control limits of 3.8297 (UCL) and 2.7843 (LCL), with the target set at 3.3070 for (A chart). The sigma is lower at 0.1742, and the difference is 1.0454.

The desired value is 0.0000, and the range of the suggested D chart is substantially less (UCL: 0.1219, LCL: -0.1219). The difference is 0.2437, and the sigma value is very modest at 0.0406.

With a difference of 1.0454, the control limit range of the proposed A chart is smaller than that of the traditional $\bar{X}$ and variance charts. Better control, process stability, and denoised data are suggested by the reduced sigma = 0.1742, which shows less variability around the target. This implies that compared to the traditional variance chart, the suggested A chart is more effective in regulating variability.

The tightest process control is indicated by the proposed D chart, which has the smallest control limit range (difference of 0.2437). Additionally, the smallest sigma, 0.0406, indicates very low variability and good precision. According to denoise data, the suggested D chart may be the most successful in attaining strict process control, and it is the most stable chart in terms of variability and range.

According to Phase II of the traditional and suggested charts in Figures 7 and 8, fresh information on infant weights was gathered for 16 samples, each with five observations, at Valia Hospital in Erbil. The new points were then calculated and displayed on the charts.

Figure 7 The fact that every point drawn on the traditional charts fell within the control boundaries indicates that the weights of the infants at Valia Hospital in Erbil were under control in terms of average and variance.

Figure 8 shows that the weights of newborns at Valia Hospital in Erbil, according to the proposed charts, were under control in terms of average and difference because all the points plotted on them fell within the control limits.

10. Conclusions

1. Overall, the new proposed charts appear to offer better control, de-noise data, lower variability, and higher precision, which is beneficial for maintaining consistent monitoring and process control.
2. The proposed D chart is the most effective chart for minimizing variability and achieving tighter control limits for all simulation cases.

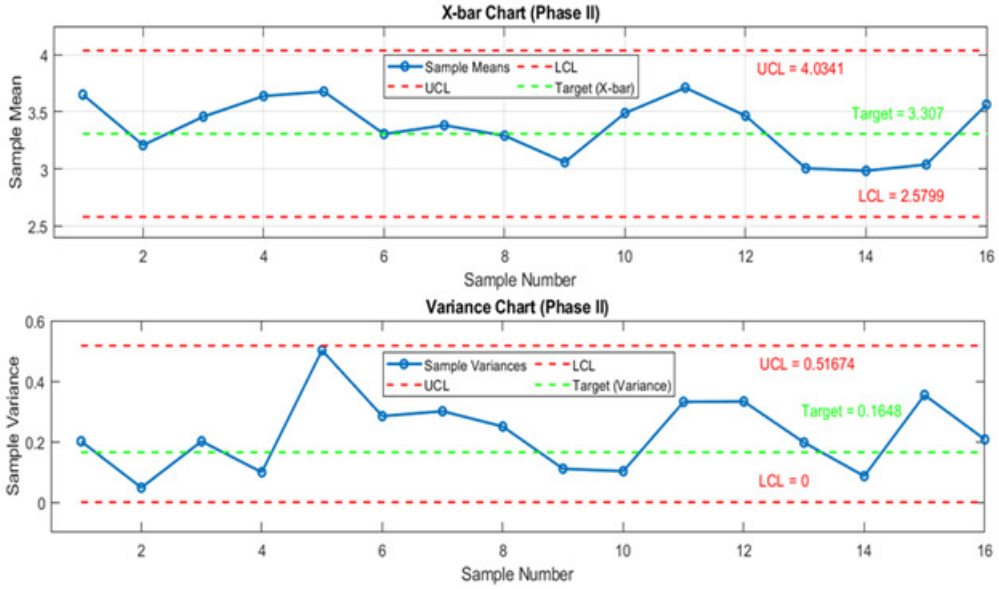

Figure 7. Classical Charts for Real Data (Phase II).

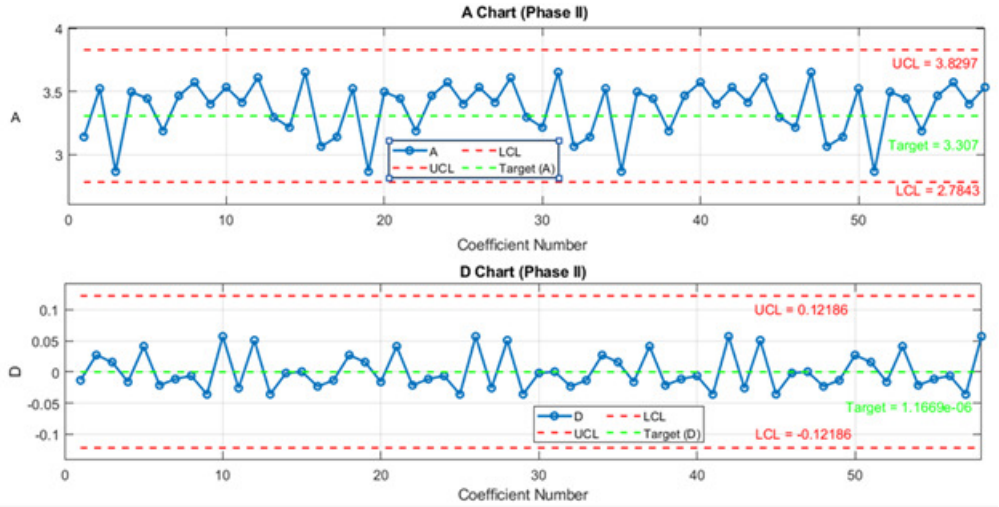

Figure 8. Proposed Charts for Real Data (Phase II).

3. The proposed A chart performs well, with tighter control than the classical methods, especially in terms of sigma and the difference between UCL and LCL for all simulation cases.
4. The classical $\bar{X}$ is useful but not as efficient in controlling and monitoring the weights of newborns at Valia Hospital in Erbil compared to the proposed charts. The classical variance charts tend to perform poorly, especially when variability (sigma) increases, due to the wide control limits and high variability.
5. The Proposed D chart is the most efficient and stable in terms of controlling variability and achieving tight process control, making it potentially the best choice for monitoring the weights of newborns at Valia Hospital in Erbil.
6. The proposed A chart also provides more efficient control compared to the classical charts, suggesting improvements over the classical $\bar{X}$ chart for monitoring the weights of newborns at Valia Hospital in Erbil.

7. The weights of newborns at Valia Hospital in Erbil were under control.

REFERENCES

1. Ali, Taha Hussien and Saleh, Dlshad Mahmood, *Proposed hybrid method for wavelet shrinkage with robust multiple linear regression model: With simulation study*, Qalaai Zanist Journal, vol. 7, no. 1, pp. 920–937, 2022.
2. Ali, Taha Hussein and Haydier, Esraa Awni, *Using Wavelet in constructing some of Average Charts for Quality control with application on Cubic Concrete in Erbil*, Polytechnic Journal, vol. 6, pp. 171–209, 2016.
3. Alt, Frank B, *Multivariate quality control*, Encyclopedia of statistical sciences, vol.8, 2004.
4. In, Francis and Kim, Sangbae, *An introduction to wavelet theory in finance: a wavelet multiscale approach*, Transactions of the Institute of Measurement and Control, vol. 44,no. 1, pp. 525–538, 2022.
5. Cohen, Achraf and Atoui, Mohamed Amine, *On wavelet-based statistical process monitoring*, World scientific, 2013.
6. Kareem, Nazeera Sedeek and Mohammad, Awaz Shahab and Ali, Taha Hussein, *Construction robust simple linear regression profile Monitoring*, Journal of Kirkuk University for Administrative and Economic Sciences, vol. 9, pp. 242–257, 2019.
7. Mallat, Stéphane, *A wavelet tour of signal processing*, Elsevier, 1999.
8. Montgomery, Douglas C, *Introduction to statistical quality control*, John wiley & sons, 2020.
9. Nason, Guy P, *Wavelet methods in statistics with R*, Springer, 2008.
10. Öz, İbrahim, *Comparative Analysis of Wavelet Families in Image Compression, Featuring the Proposed New Wavelet*, Turkish Journal of Science and Technology, vol. 44,no. 1, pp. 525–538, 2022.
11. Qader, Hogr M and Birdawod, Hawkar Q and Qader, Hevi M and Sedeeq, Bekhal S, *Capability Process to Optimize Specification by Impact of Wavelet Analysis*, Cihan University-Erbil Journal of Humanities and Social Sciences, vol. 9,no. 1, pp. 53–60, 2025.
12. Jalal, Sakar Ali and Saleh, Dlshad Mahmood and Sedeeq, Bekhal Samad and Ali, Taha Hussein, *Construction of the Daubechies wavelet chart for quality control of the single value*, IRAOI JOURNAL OF STATISTICAL SCIENCES, vol. 20,no. 1, 2024.
13. Shalby, Esraa M and Abdelaziz, Almoataz Y and Ahmed, Eman S and Abd-Elhamed Rashad, Basem, *A comprehensive guide to selecting suitable wavelet decomposition level and functions in discrete wavelet transform for fault detection in distribution networks*, Scientific Reports, vol. 15,no. 1,pp. 1160, 2025.
14. Sullivan, Joe H and Woodall, William H, *A comparison of multivariate control charts for individual observations*, Journal of Quality Technology, vol. 28,no. 4, pp. 398–408, 1996.
15. Taher, Mahmood M and Redha, Sabah Manfi, *Use The Coiflets and Daubechies Wavelet Transform To Reduce Data Noise For a Simple Experiment*, IRAOI JOURNAL OF STATISTICAL SCIENCES, vol. 19,no. 2, 2022.
16. Wierda, Sijbrand Jacobus, *Multivariate statistical process control—recent results and directions for future research*, Statistica neerlandica, vol. 48,no. 2, pp. 147–168, 1994.
17. Zakour, Sihem Ben and Taleb, Hassen, *Endpoint in plasma etch process using new modified w-multivariate charts and windowed regression*, Journal of Industrial Engineering International, vol. 13, pp. 307–322, 2017.
18. Zeroual, Abdelhafid and Harrou, Fouzi and Sun, Ying and Messai, Nadhir, *Monitoring road traffic congestion using a macroscopic traffic model and a statistical monitoring scheme*, Sustainable cities and society, vol. 35, pp. 494–510, 2017.
19. Zhang, Yanrong and Wu, Kai and Yu, Chao and Zhang, Shuang and Cai, Xiaopei, *Application of statistical process control for structural health monitoring of a high-speed railway track system*, Applied Sciences, vol. 12, no. 12, pp. 6046, 2022.